One String to Pull Them All: Fast Assembly of Curved Structures from Flat Auxetic Linkages — Supplemental Information

AKIB ZAMAN, MIT CSAIL, USA

JACQUELINE ASLARUS, MIT CSAIL, USA

JIAJI LI, MIT CSAIL, USA

STEFANIE MUELLER, MIT CSAIL, USA

MINA KONAKOVIĆ LUKOVIĆ, MIT CSAIL, USA

A Fabrication Clearance, E_{fab}

Let $\mathcal{H}(M_{2D})$ be the set of all auxetic linkages in the mesh M_{2D}. For each linkage centered at vertex $\mathbf{v}_i$, with adjacent link vertices $\mathbf{v}_j$ and $\mathbf{v}_k$, we compute the gap angle $\angle(j, i, k)$. The angle is defined as:

$$\theta = \arccos\left(\frac{(\mathbf{v}_j - \mathbf{v}_i) \cdot (\mathbf{v}_k - \mathbf{v}_i)}{\|\mathbf{v}_j - \mathbf{v}_i\| \, \|\mathbf{v}_k - \mathbf{v}_i\|}\right).$$

The total fabrication energy is:

$$E_{\text{Fab}} = \sum_{(i,j,k) \in \mathcal{H}(M_{2D})} \left\| \begin{pmatrix} \mathbf{v}_j - \mathbf{v}_i \\ \mathbf{v}_k - \mathbf{v}_i \end{pmatrix} - P_A(\mathbf{v}_j - \mathbf{v}_i, \ \mathbf{v}_k - \mathbf{v}_i) \right\|_2^2,$$

where P_A projects the vectors onto the nearest valid configuration whose angle lies within the allowed range.

$$P_A(\mathbf{v}_1, \mathbf{v}_2) = \underset{\substack{(\mathbf{x}, \mathbf{y}) \\ \theta_{\min} \leq \angle(\mathbf{x}, \mathbf{y}) \leq 90°}}{\arg\min} \left(\|\mathbf{x} - \mathbf{v}_1\|^2 + \|\mathbf{y} - \mathbf{v}_2\|^2 \right)$$

B Detailed Proof of Constraining Boundary tiles

We present a detailed proof of Theorem 5.1 in three parts. First, we establish the rigidity of a single unit tile in our system using Maxwell's framework. Second, we give a general proof for regular topologies of $N \times N$ tiling (square) and $N \times M$ rectangular grid introducing Lemma B.1. Finally, we introduce Lemma B.2 and prove the corresponding result for irregular topologies.
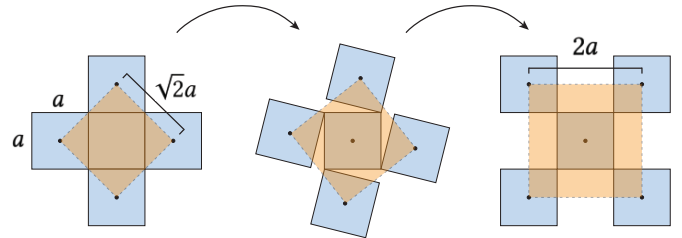
Fig. 18. Illustration of quad auxetic linkage expansion from fully closed to maximally extended. The linkage expands to cover twice as big an area, as illustrated by the orange bounding box.
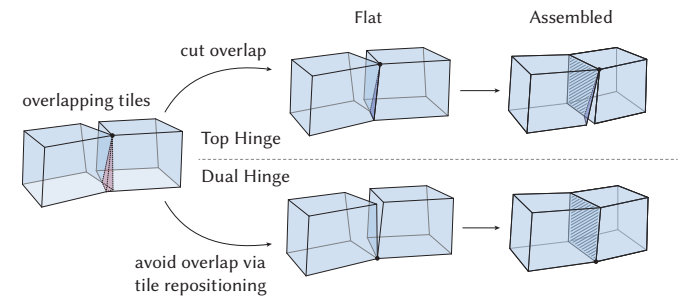

Fig. 19. Regions of negative curvature will create tiles that overlap in the flat configuration. To maintain a top hinge connection, the overlapping region (highlighted with red) must be cut to achieve fabricability, which leads to a partial contact between side faces in the assembled state (contact between tiles is highlighted with dashed lines). By placing the hinge on the bottom vertices, overlap is avoided and complete contact between the side faces is enabled in the assembled state.

B.1 Preliminaries

Maxwell's Count. Maxwell's count [Lubensky et al. 2015] provides a necessary combinatorial condition for the infinitesimal rigidity of a bar-and-joint framework in d dimensions. If the framework has:

- n joints (nodes), each with d translational degrees of freedom, and
- b bars (edges), each imposing one length constraint,

then a necessary condition for infinitesimal rigidity is:

$$b \geq dn - \frac{d(d + 1)}{2} \tag{7}$$

• Zaman, Aslarus, Li, Mueller, Konaković Luković

where, dn is the total number of independent displacement variables and $\frac{d(d+1)}{2}$ is the number of rigid-body degrees of freedom in d dimensions. When equality holds with no redundant constraints, the framework is called *isostatic* or a *Maxwell frame*. In particular, for $d = 2$, one obtains $b \geq 2n - 3$, and for $d = 3$, $b \geq 3n - 6$.

The rigidity of an eight-vertex quadrilateral frustum is well studied in structural engineering [Kem 2015]. Since each unit tile in our mechanism is such a frustum, Maxwell's count predicts it requires $3 \times 8 - 6 = 18$ bars to be rigid. To be exact, they consist of 12 edge-length bars (4 around the bottom face, 4 around the top face, and 4 vertical edges) plus 6 no-shear diagonal bars (one on each of the six faces) [Kem 2015].

Edge Constraints. In $\mathbb{R}^3$, each quadrilateral frustum tile $T = \{v_1, \ldots, v_8\}$ requires 18 fixed length bars to be rigid under Maxwell's count. Each bar between vertices v_i and v_j imposes the holonomic constraint

$$g_{\text{edge}}(v_i, v_j) = \|v_i - v_j\|^2 - d_{ij}^2 = 0,$$

where d_{ij} is the prescribed distance between those two vertices. A tile with n bars thus contributes n such scalar constraints to the rigidity matrix.

Link Constraints. Each hinge forces two vertices between two tiles to coincide spatially. We model each link between two nodes v_i and v_j as a link constraint,

$$v_i - v_j = 0$$

which can be written as

$$g_{\text{link},x}(v_i, v_j) = v_{i,x} - v_{j,x} = 0,$$
$$g_{\text{link},y}(v_i, v_j) = v_{i,y} - v_{j,y} = 0,$$
$$g_{\text{link},z}(v_i, v_j) = v_{i,z} - v_{j,z} = 0.$$

Since these constraints enforce vertex coincidence (not fixed lengths), each hinge contributes three independent scalar constraints. Hence, with n hinges in the system, there are in total $3n$ link constraints.

B.2 Calculating Degree of Freedom (DoF)

We show that adding a single link constraint can reduce the total DoF by anywhere from 0 to 3 (see Figure 20). Let's consider a simple example of two tiles: each tile has 6 DoF (three translational and three rotational), so together they have 12 DoF. Now, as we sequentially add four hinge-links at the vertices of their shared side face, we observe the following reductions in the DoF of the system:

- The first link (Figure 20a) fixes one vertex in all three translational directions, reducing the total DoF from 12 to 9 (change of 3)
- the second link (Figure 20b) removes two rotational DoF (tilt about two axes) from one of the tiles, bringing the count to 7 (change of 2)
- the third link (Figure 20c) eliminates the remaining rotational DoF (spin about the final axis), further reducing it to 6 (change of 1)
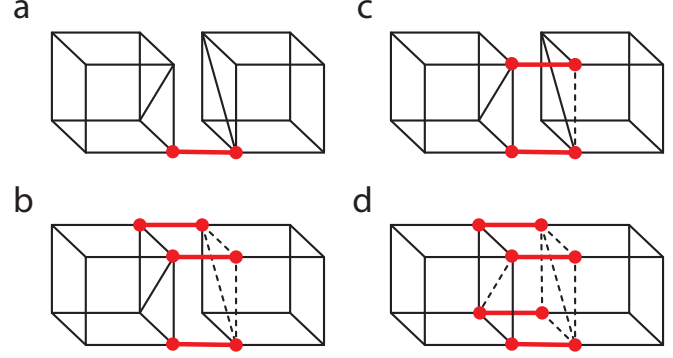- the fourth link (Figure 20d) doesn't change the DoF of the system anymore (change of 0)

Fig. 20. Sketch of vertex position constraints (red) applied to two tiles. The resulting redundant edge length constraints are shown with dotted lines.

Figure 20a illustrates a fully independent case, where all of the constraints are independent, and removing any constraint will result in extra DoF(s). However, Figure 20b-d highlights how, after adding link constraints, some of the edge-length constraints (marked by *black dashed lines*) become redundant. To compute the framework's DoF correctly, we followed the formulation of [Chen et al. 2020].

Let, N denote the total number of vertices and thus the total independent variables in the system, $V = 3N$. If there are total M constraints (combining edge length and link constraints), each constraint can be written as $g(x) = 0$, where g is a function of the V coordinates of all nodes N. We then define the rigidity matrix, A to be :

$$A \in \mathbb{R}^{M \times V}, \qquad A_{ij} = \frac{\partial g_i(x)}{\partial x_j},$$

To determine the DoF of the system from the rigidity matrix A, we subtract the number of independent constraints from V as:

$$\text{DoF} = V - \text{rank}(A).$$

Now, if there are E independent edge length constraints and L independent hinge (link) constraints, then $\text{rank}(A) = E + L$, so

$$\text{DoF} = V - (E + L) \qquad (8)$$

B.3 Proof of Theorem 5.1

In Theorem 5.1, we state: A linkage formed of eight-vertex quadrilateral-frustum rigid tiles in $\mathbb{R}^3$, each joined to its neighbors at a single corner and arranged so that every interior void is a four-vertex rhomboid, when enclosed by and tensioned with a single continuous boundary string, is isostatic, admitting exactly the six trivial rigid-body motions and no internal infinitesimal flexes.

In this proof, in a quad auxetic topology, tiles with at least one vertex on the boundary loop are termed *boundary tiles* and all others are *internal tiles*. Without string placed in the boundary, Vertex-to-Vertex Links are of two types:

- *Internal links.* Create link constraints between either two internal tiles or an internal tile to a boundary tile
- *Boundary links.* Create link constraints between pairs of boundary tiles and are situated at the boundary loop of the structure.
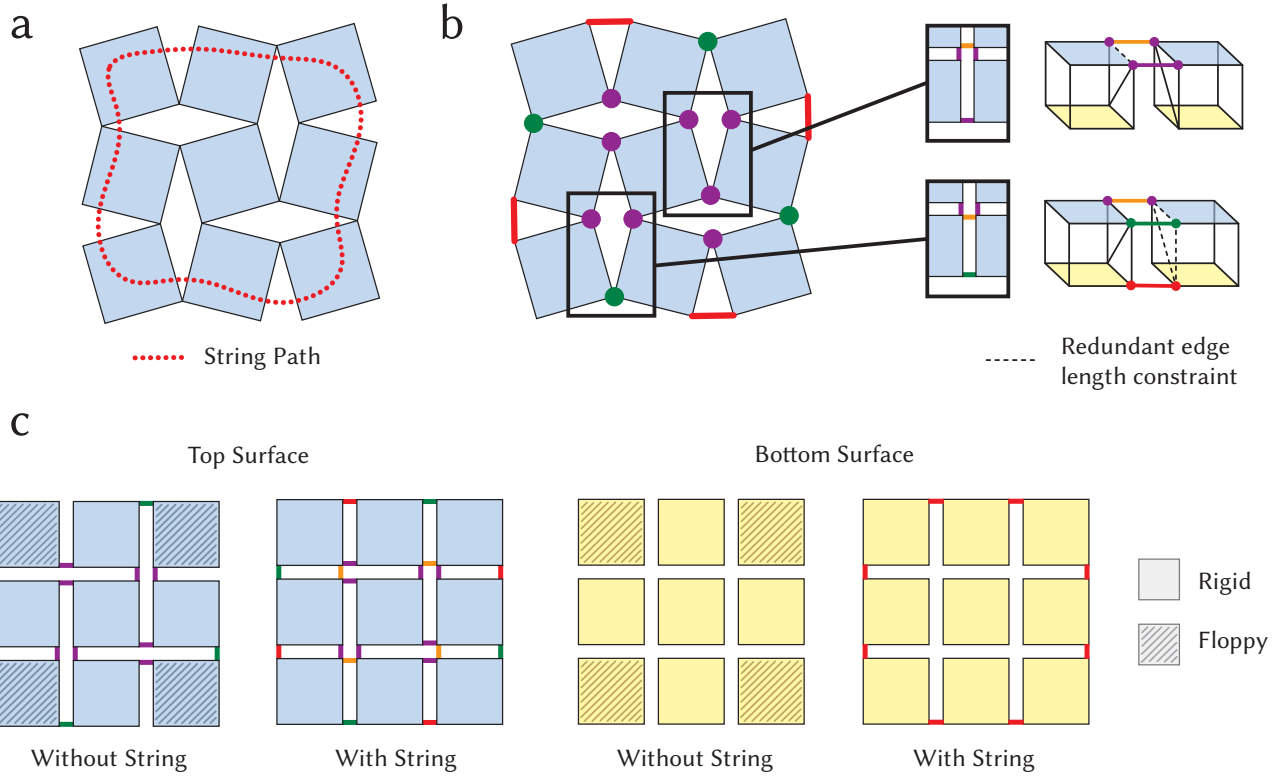
Fig. 21. (a) Illustration of the string path to constrain the boundary of a 3x3 pattern. (b) Illustration of resulting constraints. Purple depicts internal hinges and green depicts boundary hinges. Inset shows redundant edge length constraints that result from imposed link constraints. (c) Diagram of top and bottom faces of the linkage. Colored lines depict the constraints the type of constraint between two vertices.

We refer to Figure 21 for a visualization of this system in a 3×3 tile assembly, where each tile is a quadrilateral frustum with eight vertices and six faces.

Figure 21a shows the string path around the boundary tiles. Figure 21b shows the links, where purple dots are internal links, and green dots are boundary links. Additionally, for a simpler visualization, we provide a 2D view of the *top* and *bottom* surface (see Figure 21c) of the mechanism, where the links are represented as solid line matching the color scheme of Figure 21b.

For a $N \times N$ pattern (Square Grid), there are total N^2 tiles, each having 8 vertices. Thus, the total number of variables when $d = 3$ is

$$V = d \cdot 8 \cdot N^2 = 24N^2$$

Now, there are $2(N - 1)^2$ internal links and $2(N - 1)$ boundary link following the quad auxetic topology, each imposing 3 scalar constraints. Thus, the total independent scalar constraints due to internal links (I) and boundary links (B) is:

$$I = 3 \cdot 2 (N - 1)^2 = 6 (N - 1)^2,$$

$$B = 3 \cdot 2 (N - 1) = 6 (N - 1)$$

Now referring to Figure 21a, when the string is routed inside the tiles along the path, it exits one tile and then enters the next at a position within the interior of the side face. This effectively pulls the adjacent side faces together when the string is tensioned. In practice there may

be slight fabrication errors at the string crossings, but here we assume perfect closure and ideal tension. We model this phenomenon of spatial constraining due to string tension as an additional link constraint between the involved vertices. Please note that in our system all side faces are kept planar and held in full contact with their neighbors during the shape encoding of the tiles (see Section 4.2 in Main Text)

As the string wraps around the boundary loop and is tensioned, it "glues" together the corresponding opposite internal-link pairs on either the top or bottom surface, shown by red dashed lines. Each dashed-line constraint adds exactly one independent restriction (along the string's tension axis), since the paired vertices are already fixed in all three axes by their original link. So, in Figure 1B, all solid lines except *orange* shows the location of the link constraints which contribute 3 independent scalar constraints to the system.

We now focus on the region outlined by the orange lines in Figure 22, isolating just two tiles that share this exact configuration. If a string is routed through the boundary (see Figure 22), it constrains two of the four vertex pairs (a and b) on the adjacent side faces of the neighboring tiles. We then ask: does constraining one of the remaining pairs (c or d) still require three independent scalar constraints, or can it be achieved with fewer?

LEMMA B.1. *If two rigid frustum tiles are linked along an edge at both vertices (in all three coordinate axes), then imposing a link between*
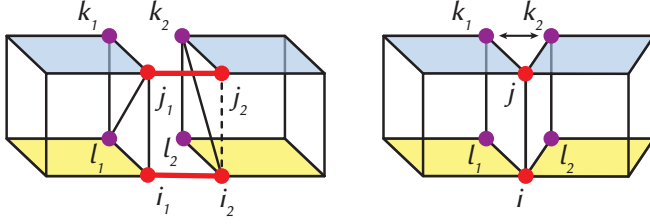
Fig. 22. This figure highlights the key insight of Lemma B.1: when two tiles are connected at vertices along one shared edge, motion is constrained to one axis. Top and bottom faces are denoted with blue and yellow, respectively.

a third vertex pair that shares an edge with either of the previously constrained vertices introduces one independent constraint in the Rigidity Matrix (i.e. removes only one DoF).

PROOF. Referring to Figure 22, the two tiles together have $2 \times 6 = 12$ DoF. As shown in Section B.2, fully constraining vertex pairs a and b in all three coordinates (x, y, z) removes five DoF (three translational and two rotational), changing the overall DoF from 12 to 7. Hence, with the current set of scalar constraints in the system intact, any additional link at either c or d can never eliminate more than one DoF, yielding a final count of 6. □

Now we calculate all the link constraints which are being imposed by the string tension. For simplicity, we have considered all of the hinges on top. Please note that, during hinge placement (see Section 4.4) hinges have been placed on either top or bottom, thus this formulation works for any topology of our system. Now, there always exists the same number of string segments as the boundary links $2(N-1)$. The string is pulling both top and bottom vertices in those connecting string segments (see Figure 22) creating $2 \cdot 2 (N-1)$ each contributing 3 scalar constraints. Similarly, the bottom vertices of the boundary links are also being constrained by the string creating additional $2(N-1)$ links. On top of that, from each boundary link facing inside of the structure, we get additional $2(N-1)$ links (following Lemma B.1) , each of which contribute only one scalar independent constraint rather than three. Thus the independent scalar constraints added due to string pull:

$$S = 3 \cdot 2 \cdot 2 (N-1) \; + \; 3 \cdot 2 (N-1) \; + \; 2 (N-1) = 20 (N-1)$$

Thus, total independent link constraints, L is as follows:

$$\begin{aligned} L &= I + B + S \\ &= 6(N-1)^2 + 6(N-1) + 20(N-1) \\ &= (N-1)(6N+20) \\ &= 6N^2 + 14N - 20, \end{aligned}$$

Now, for N^2 tiles, there are total $18N^2$ independent edge constraint. However, when you place the link constraints, the number of redundant edge constraint is as follows:

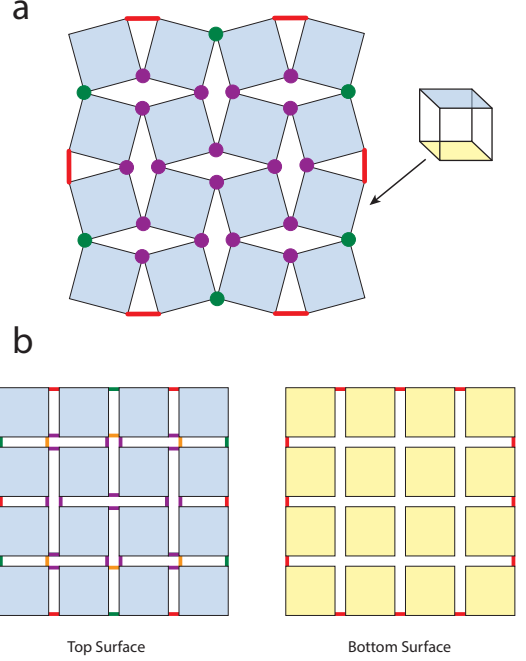$$R = 3 \cdot 2 \cdot 2 (N-1) + 2 (N-1) = 14 (N-1),$$

Fig. 23. (a) Illustration of the string path to constrain the boundary of a 4x4 pattern. (b) Diagram of top and bottom faces of the linkage. Colored lines depict the constraints the type of constraint between two vertices.

where $3 \cdot 2 \cdot 2 (N-1)$ are the redundant edges in the boundary tiles as marked and $2 (N-1)$ are the redundant edges in the internal tiles which is always equal to the number of boundary links. Thus, total independent edge constraint, E' is:

$$E' = E - R = 18 N^2 - 14 N + 14,$$

Thus, from Equation 8, we get,

$$\begin{aligned} \text{DoF} &= V \; - \; E' \; - \; L \\ &= 24 N^2 \; - \; \left(18 N^2 - 14N + 14\right) \; - \; \left(6N^2 + 14N - 20\right) \\ &= 6. \end{aligned}$$

According to this formulation, for $N = 3$ (see Figure 21):

$$V = 216, \; I = 24, \; B = 12, \; S = 40, \; L = 76, \; E = 162, \; R = 28$$
$$DoF = 216 - (162 - 28) - 76 = 6$$

for $N = 4$ (see Figure 23):

$$V = 384, \; I = 54, \; B = 18, \; S = 60, \; L = 132, \; E = 288, \; R = 42$$
$$DoF = 384 - (288 - 42) - 132 = 6$$

Similarly for $N \times M$ (rectangular grid), there are total $N \cdot M$ tiles. Considering the same notations, we find that the DoF for rectangular topology is also 6 while being tensioned by the string.

$$T = NM$$

$$V = d.8.T = 3.8.NM = 24NM$$

$$I = 3.2(N-1)(M-1) = 6(N-1)(M-1)$$

$$B = 3\{(N-1)+(M-1)\} = 3(N+M-2)$$

$$S = 3.2(N+M-2) + 3(N+M-2) + (N+M-2)$$

$$= 10(N+M-2)$$

$$L = 6(N-1)(M-1) + 3(N+M-2) + 10(N+M-2)$$

$$= 6(N-1)(M-1) + 13(N+M-2)$$

$$= 6NM + 7N + 7M - 20$$

$$E = 18NM$$

$$R = 3.2(N+M-2) + (N+M-2) = 7(N+M-2)$$

$$E' = E - R$$

$$= 18NM - 7N - 7M + 14$$

$$DoF = V - E' - L$$

$$= 24NM - \left(18NM - 7N + 7M + 14\right) - \left(6NM + 7N + 7M - 20\right)$$

$$= 6$$

According to this formulation, for the case of a 4×5 linkage (see Figure 24):

$$V = 480, \ I = 72, \ B = 21, \ S = 70, \ L = 163, \ E = 360, \ R = 49$$

$$DoF = 480 - (360 - 49) - 163 = 6$$

Consider a particular quadrilateral negative void in Figure 25b, annotated with tile numbers (T_1, T_2, T_3 and T_4). The 2D view of the top-faces of these tiles are illustrated in Figure 25c and the corresponding 3D view in Figure 25d.
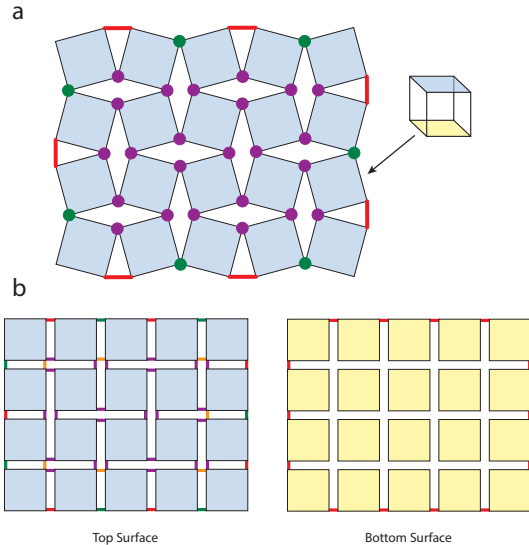

Fig. 24. (a) Illustration of the string path to constrain the boundary of a 4x5 pattern. (b) Diagram of top and bottom faces of the linkage. Colored lines depict the constraints the type of constraint between two vertices.

LEMMA B.2. *For a void bounded by four frustum tiles in a quad auxetic topology, the two vertices on the shorter diagonal will work as a link (i.e. coincide) without contributing any independent constraint in the Rigidity Matrix if either of the adjacent gaps sharing the those vertices are linked at top and bottom, and the neighboring tiles at the remaining two vertices are linked at the top surface with at least one of them also linked at the bottom surface.*

PROOF. In a quad auxetic topology, we have four quadrilateral-frustum tiles T_1, T_2, T_3, and T_4 arranged around a common quadrilateral void g_1, with vertex-pair contacts labeled v_{12}, v_{23}, v_{34}, v_{14}. g_2 and g_3 are the adjacent gaps around g_1. Two vertices on the shorter diagonal are v_{12} and v_{34}. If either of the adjacent gaps g_2 and g_3, are linked at the top and bottom, then all in-plane translations and rotations of the associated tiles are eliminated, leaving only a single DoF: an out-of-plane translation involving the opposite vertex pair $\{v_{23}, v_{14}\}$. When both $\{v_{23}, v_{14}\}$ are linked at the top and at least one of them is also linked at the bottom, the remaining DoF is eliminated, forcing v_{12} and v_{34} to coincide in all three axes. This coincidence effectively acts as a hinge link without adding an independent constraint to the rigidity matrix. □

In plain words, four frustum tiles are arranged around a four-sided void. Fully clamping two opposite contact points on one face, fixing them both on the top surface and at least one on the bottom, eliminates all in-plane translations and rotations of those tiles. Finally, adding a single clamp at one of those remaining corners, again both above and below removes that last degree of freedom, causing that other pair of corners to coincide without requiring any further constraints.

Following the formulation of Lemma B.2, for an irregular 6-tile linkage (see Figure 26):

$$V = 144, \ I = 6, \ B = 12, \ S = 36, \ L = 54, \ E = 108, \ R = 24$$

$$DoF = 144 - (108 - 24) - 54 = 6$$

Similarly, for an irregular 8-tile linkage (see Figure 25):

$$V = 192, \ I = 18, \ B = 12, \ S = 38, \ L = 68, \ E = 144, \ R = 26$$

$$DoF = 192 - (144 - 26) - 68 = 6$$

Similarly, for an irregular 16-tile linkage (see Figure 27):

$$V = 384, \ I = 48, \ B = 21, \ S = 66, \ L = 135, \ E = 288, \ R = 45$$

$$DoF = 384 - (288 - 45) - 135 = 6$$

C Finding Dominant Peaks and associated Basins

C.1 Graph Formulation

For each gap G_i, let $\mathcal{T}(G_i)$ be the set of surrounding tiles, where each tile $t_k \in \mathcal{T}(G_i)$ has mass m_k and center-of-mass height z_k. Let $z_{\min}$ denote the lowest point in the structure. The gap's gravitational potential energy (GPE), g_i, is given by:

$$g_i = \sum_{t_k \in \mathcal{T}(G_i)} \frac{1}{4} m_k \, g \, (z_k - z_{\min}).$$

Fig. 25. (a) Illustration of the string path to constrain the boundary of an irregular 8-tile pattern. (b) Illustration of resulting constraints. Purple depicts internal hinges and green depicts boundary hinges. Inset shows redundant edge length constraints that result from imposed link constraints. (c) Diagram of top and bottom faces of the linkage. Colored lines depict the constraints the type of constraint between two vertices.
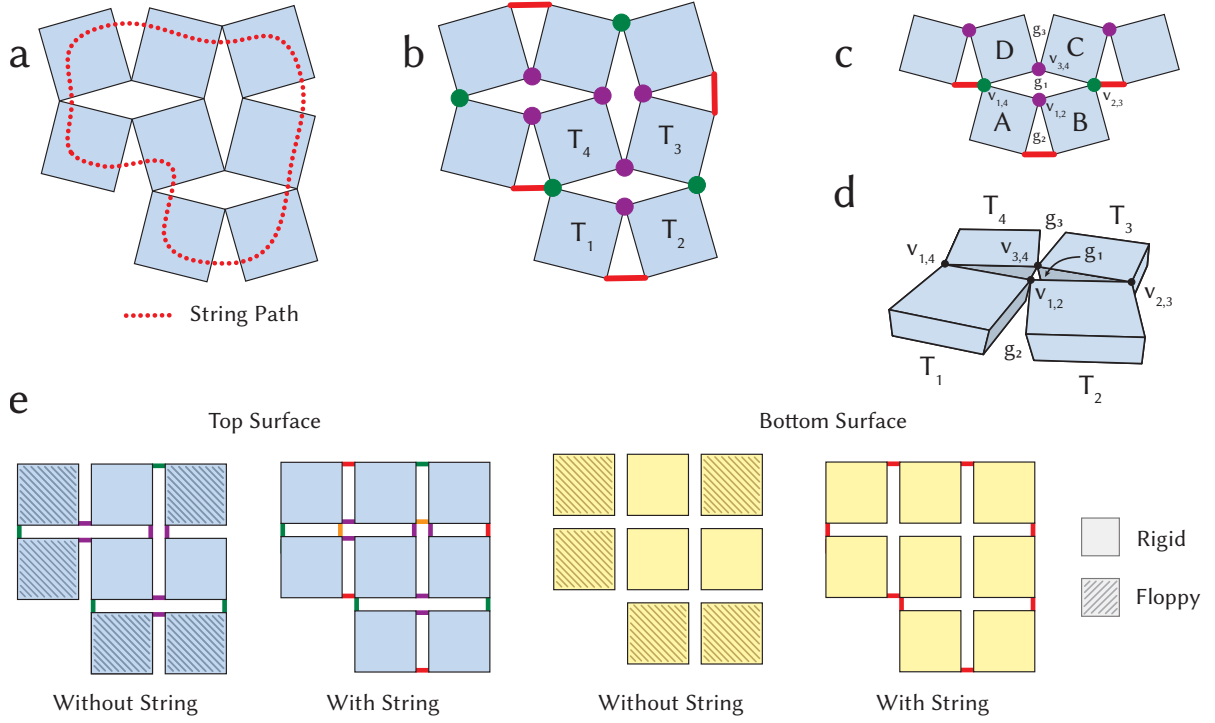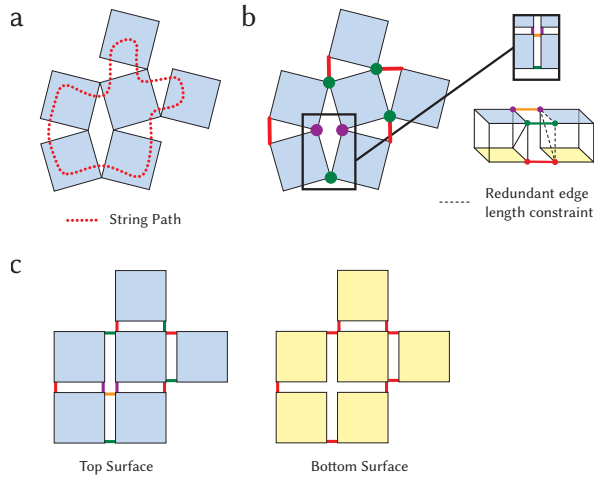

Fig. 26. (a) Illustration of the string path to constrain the boundary of an irregular 6-tile pattern. (b) Illustration of resulting constraints. Purple depicts internal hinges and green depicts boundary hinges. Inset shows redundant edge length constraints that result from imposed link constraints. (c) Diagram of top and bottom faces of the linkage. Colored lines depict the constraints the type of constraint between two vertices.
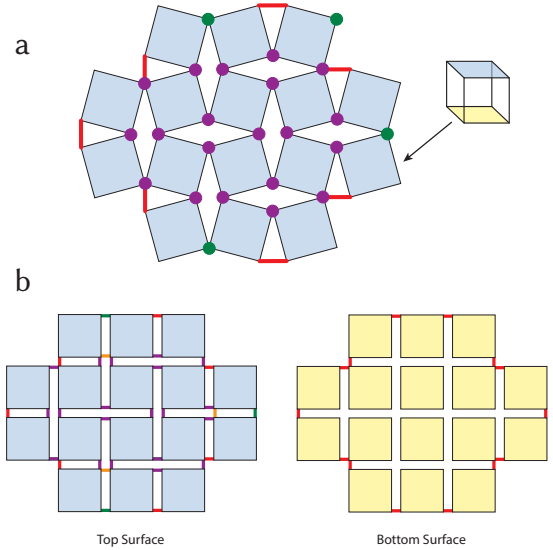

Fig. 27. (a) Illustration of the string path to constrain the boundary of an irregular 16-tile pattern. (b) Diagram of top and bottom faces of the linkage. Colored lines depict the constraints the type of constraint between two vertices.

We build a weighted graph (V, E) of gaps, where each node $v_i \in V$ corresponds to a gap G_i, and each edge $e_{i,j} \in E$ indicates that two gaps share a vertex within the auxetic mesh. We assign each node with the weight g_i.

C.2 Finding Peaks

The discrete gradient per gap on this graph can be defined as:

$$\nabla g_i = \arg \max_{j \in N(i) \cup \{i\}} g_j$$

where $N(i)$ is the neighbor set of gap i. Peaks are the gaps with no higher neighbor, defined as:

$$P = \{i \in V : \nabla g_i = i\}$$

C.3 Finding Associated Basins

For each peak $p \in P$, the basin of attraction is the set of gaps that converge to p under gradient ascent. Let V be the set of gaps, and $\nabla g(i)$ the gradient ascent mapping from gap i to its steepest-ascent neighbor. Repeated application is written as $\nabla g^{(k)}(i)$. Then

$$\text{Basin}(p) = \{\, i \in V : \exists\, k \geq 0 \;\; \nabla g^{(k)}(i) = p \,\}, \qquad p \in P,$$

i.e., all gaps whose gradient-flow path ends at p. The total basin energy is the sum of their gap potential energies:

$$G_{\text{Basin}}(p) = \sum_{i \in \text{Basin}(p)} g_i.$$

D Derivation of E_{Channel}

The infinitesimal work dW done against friction, F_{Fric} over a small wrap angle $d\theta$ is:

$$dW = F_{\text{Fric}}\, ds = \big(\mu_c\, N(\theta)\big)\, (R\, d\theta),$$

where, μ_c is the channel-wall friction coefficient, $N(\theta)$ is the normal force pressing the rope into the channel at angle θ, R is the (assumed constant) local bend radius, and $R\, d\theta$ is the arc-length. Since the local normal equals the local tension divided by the radius, $N(\theta) = \frac{T(\theta)}{R}$, we get:

$$dW = \mu_c\, \frac{T(\theta)}{R}\, (R\, d\theta) = \mu_c\, T(\theta)\, d\theta.$$

By the Capstan (belt-friction) law [Stuart 1961],

$$T(\theta) = T_1\, e^{\mu_c\, \theta},$$

where T_1 is the entry-tension at $\theta = 0$. Substituting this into the work integral and integrating from $\theta = 0$ to $\theta = \theta_{\text{Total}}$ gives

$$E_{\text{Channel}} = \int_0^{\theta_{\text{Total}}} \mu_c\, T_1\, e^{\mu_c\, \theta}\, d\theta = T_1 \left[e^{\mu_c\, \theta_{\text{Total}}} - 1 \right].$$

Hence the total frictional energy loss in the channel is

$$\boxed{E_{\text{Channel}} = T_1 \big(e^{\mu_c\, \theta_{\text{Total}}} - 1 \big).}$$

E Actuation Simulation Details

n indexes discrete time steps: $t_n = n\, \Delta t$ with fixed step, $\Delta t > 0$. Thus $\mathbf{x}_i^n$ and $\mathbf{v}_i^n$ denote the position and velocity of vertex i at time t_n, and the lumped mass at vertex i is $m_i > 0$. At each step, we solve an optimization that outputs the updated position of vertex i balancing (i) staying close to the predicted location of vertex i under its current velocity and acceleration due to external force, $\mathbf{F}_{\text{ext}}$ (ii) satisfying the geometric constraints (e.g. rigidity, non-collision and actuation requirements) involving vertex i. We then update the velocity using linear damping with factor $\gamma \in [0, 1]$ and the same acceleration. The updated position of vertex i at $t_{n+1} = t_n + \Delta t$ is defined as:

$$\mathbf{x}_i^{n+1} = \arg \min_{\mathbf{x}_i} \left(\tfrac{1}{2} \left\| \mathbf{x}_i - \mathbf{x}_i^{\text{pred}} \right\|^2 + \sum_j w_j\, E_j(\mathbf{x}_i) \right),$$

where, x_i refers to a vertex in the linkage and $E_j(\mathbf{x}_i)$ represents the energy with corresponding weight w_j associated with each geometric constraints on that vertex. The predicted location $\mathbf{x}_i^{\text{pred}}$ of vertex i under its current velocity and acceleration due to external force, is calculated as:

$$\mathbf{x}_i^{\text{pred}} = \mathbf{x}_i^n + \Delta t\, \mathbf{v}_i^n + \Delta t^2\, \mathbf{a}_i^n, \qquad \mathbf{a}_i^n = \frac{\mathbf{F}_{\text{ext},i}^n}{m_i},$$

Then, we update the velocity at $t_{n+1} = t_n + \Delta t$ as:

$$\mathbf{v}_i^{n+1} = (1 - \gamma)\, \mathbf{v}_i^n + \Delta t\, \mathbf{a}_i^n.$$

Snap constraint, E_{Snap}. The *snap* constraint forces the mid-points of paired side faces to coincide, thereby closing each gap along the string path:

$$E_{\text{Snap}} = \sum_{m \in M(T_{2D})} \left\| \mathbf{x}_m - P_{\text{Snap}}(\mathbf{x}_m) \right\|_2^2, \tag{9}$$

where $M(T_{2D})$ is the set of mid-points on the string path in the flat layout T_{2D}, $\mathbf{x}_m$ denotes the current 3-D position of midpoint m, and the projection operator $P_{\text{Snap}}(\mathbf{x}_m)$ returns the current position of its paired midpoint on the neighboring tile. Minimizing E_{Snap} drives each midpoint to its partner, collapsing every gap without explicitly modeling the string's bending or dynamics.

Lift constraint, E_{Lift}. The *lift* constraint ensures that the string's exit point raises each designated gap to its prescribed 3-D position. We formulate

$$E_{\text{Lift}} = \sum_{l \in L} \left\| \mathbf{x}_l - P_{\text{Lift}}(\mathbf{x}_l) \right\|_2^2,$$

where L is the set of lift-point indices, $\mathbf{x}_l \in \mathbb{R}^3$ is the current position of lift point l, and the projection operator $P_{\text{Lift}}(\mathbf{x}_l)$ returns its target position in the assembled configuration. Minimizing E_{Lift} drives each lift point to its correct height.

Table 1. Mass and dimensions of fabricated results, rounded to the nearest integer unit

Model	Mass (g)	2D Length (mm)	2D Width (mm)	3D Length (mm)	3D Width (mm)	3D Height (mm)
Chair	96	289	75	128	70	93
Lilium	176	211	212	169	165	42
Train Station	93	175	128	166	109	24
Igloo	175	240	214	195	143	63
Human-scale Chair	8369	2794	476	848	422	978